

Supplemental Material: Speckle engineering through singular value decomposition of the transmission matrix

Louisiane Devaud,^{1,*} Bernhard Rauer,¹ Jakob Melchard,² Matthias Kühmayer,² Stefan Rotter,² and Sylvain Gigan¹

¹*Laboratoire Kastler Brossel, ENS-Université PSL, CNRS,*

Sorbonne Université, Collège de France, 24 rue Lhomond, 75005 Paris, France

²*Institute for Theoretical Physics, Vienna University of Technology (TU Wien), A-1040 Vienna, Austria*

(Dated: July 28, 2021)

I. EXPERIMENTAL DETAILS

I.1. Geometry of illumination and detection

As indicated in Fig. 1 of the main text, the phase pattern on the SLM is imaged onto the back focal plane of the illumination objective such that the input surface of the scattering media is close to the Fourier plane of the SLM. However, as presented in Fig. S1, we slightly defocus the illumination objective by a fixed distance $|z_{\text{obj}_1}| = 0.5$ mm to increase the illuminated area to a diameter of $d \simeq 280$ μm . As the medium's thickness is comparatively small ($\simeq 10$ μm), the area at which the light exits the medium is approximately the same as the illumination area. On the camera, its image covers the whole CCD such that different realizations can be obtained simply by choosing different regions around the center of the image. The magnification of the imaging system is 22.2.

On the output surface, the extent of the illuminated area together with the distance z at which the speckle is observed determine the speckle grain size (given a blank input pattern is displayed on the SLM) [1]. In the experiment, the limited NA of the collection objective influences the grain size as well. These features are best observable in Fourier space, revealing the spatial frequencies present in the patterns. Fig. S1 (bottom part) shows the Fourier transformed speckle patterns at three imaging planes along the z direction. Imaging the speckles right at the medium output surface, the observed spatial frequencies are only limited by the NA of the objective, leading to a flat top distribution. Moving the imaging plane away from the medium, the limited exit surface of the light becomes dominant and the distribution gets peaked at low spatial frequencies, corresponding to an increase of the speckle grains.

For the measurements performed with an inhomogeneous speckle Fourier distribution, as in Fig. 2 and Fig. 4(c) of the main text, we image a plane at a distance $z \simeq 1$ mm behind the medium. For the data presented in Fig. 3 and Figs. 4(a-b) a plane close to the medium output surface was imaged.

I.2. Ratio of controlled and detected modes

The measured TMs have the dimension $N_{\text{CCD}} \times N_{\text{SLM}}$, where N_{CCD} is the number of pixels in the region-of-interest on the CCD and N_{SLM} is the number of input modes controlled by the SLM. For the measurements presented in Fig. 2 and Fig. 4(c) of the main text $N_{\text{SLM}} = 1024$ and $N_{\text{CCD}} = 225$ while for the measurements of Fig. 3 and Figs. 4(a,b) $N_{\text{SLM}} = 4096$ and or $N_{\text{CCD}} = 900$. However, these numbers do not directly translate to the number of controlled and measured modes. Due to the intentional oversampling of the measured speckles the output patterns contain fewer independent modes, specifically 100 for the smaller region-of-interest and 400 for the larger. Furthermore, circular beam clipping at the illumination objective's back focal plane cuts the modes at the edges of the square region controlled on the SLM, see Fig. S1. Therefore, only about 80% reach the scattering medium. This results in an output-to-input control ratio of 0.2 for all measurements presented.

To reach the previous control values some experimental precautions are taken. The modulated SLM region covers the light beam to avoid non modulated co-propagating light. Thus SLM pixels are grouped to form macropixels (of 10×11 pixels for 1024 modes). Also, due to the magnification, a single speckle grain covers several CCD pixels. When measuring the TM the images are binned. For the data of Fig. 2, after a binning of 3×3 pixels, a speckle grain corresponds to two CCD pixels to fulfill the over-sampling condition.

* louisiane.devaud@lkb.ens.fr

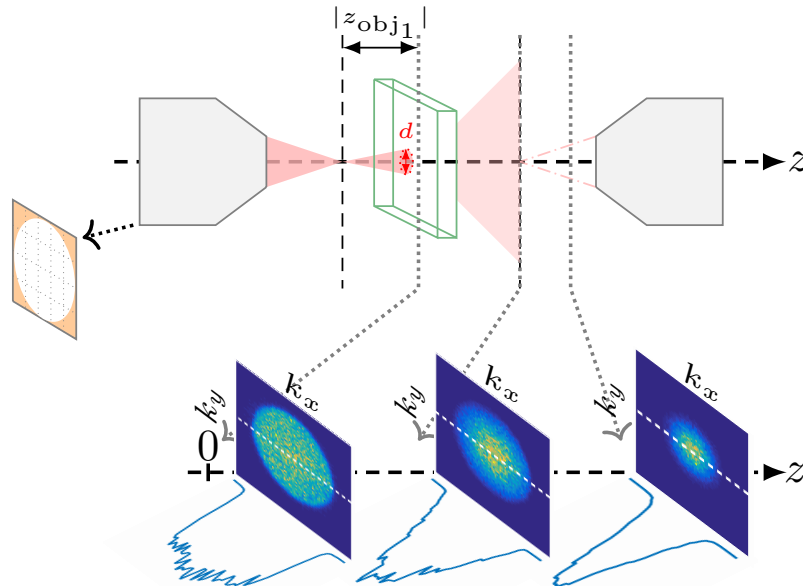


FIG. S1. Top: illumination and collection geometry. The first microscope objective is defocused by $|z_{\text{obj}1}| = 0.5$ mm giving an illuminated area of $\pi d^2/4 = 0.06$ mm². The scattering medium thickness is about 10 μm . The SLM is imaged on the back focal plane of the illumination microscope objective such that its circular aperture cuts off the modes at the edge of the controlled region (on the orange region). The imaged plane is at a varying distance z from the sample. Bottom: spatial frequency distribution of speckles for different imaging planes behind the medium surface (positioned at $z = 0$). The imaged planes are, from left to right: $z \simeq 0$, $z \simeq 0.8$ and $z \simeq 1.2$ mm. Corresponding central cuts through the distributions are shown below. The shown data is obtained by averaging over 20 realizations of random input patterns displayed on the SLM.

II. MINIMAL MODEL FOR THE GRAIN SIZE CONTROL

In order to better understand the results on the speckle grain size control reported in the main text we devise a simple model that convincingly reproduces the experimental results. First, we generate a fully random TM with independent and identically complex Gaussian distributed elements. Then we take each column of this TM corresponding to the output image for a given input pixel and impose local correlation. For that we reshape the column values into a 2D image and convolve it with a Gaussian whose width defines the spatial correlation length, i.e. the speckle grain size. Applying this convolution process to each 2D image and reshaping them back to single columns gives us the correlated TM.

For this correlated TM, we can now perform the SVD and calculate the output speckle patterns corresponding to the individual singular vectors, in analogy to the experiment. Fig. S2(b) shows the distribution of spatial frequencies for the output field of three of those vectors using phase and amplitude information while Fig. S2(c) shows the same with only the phase of the singular vectors being projected. In the second case, the results are in good agreement with the experimental findings shown in Fig. 2(b) of the main text. Also, the extracted grain size presented in Fig. S2(c) agrees well with the experimental observations in the case of phase-only control.

The Gaussian form of the local correlations used in this minimal model does not fully reflect the experimental grain size correlations. Nevertheless, the model shows that nothing more than local correlations that result in a non-uniform distribution of spatial frequencies is needed for the effect to appear. Important to note is that the phase-only restriction does not affect much the output for the first singular vectors. We attribute this to the fact that the first singular vectors are transmitted better, enhancing their contribution compared to the background created by not displaying the full singular vector.

III. SPECKLE STATISTICS

The field amplitude statistic of a fully developed speckle pattern follows a Rayleigh distribution while its phase is uniformly distributed between $-\pi$ and π . In the main text we pointed out small deviations from this behaviour for

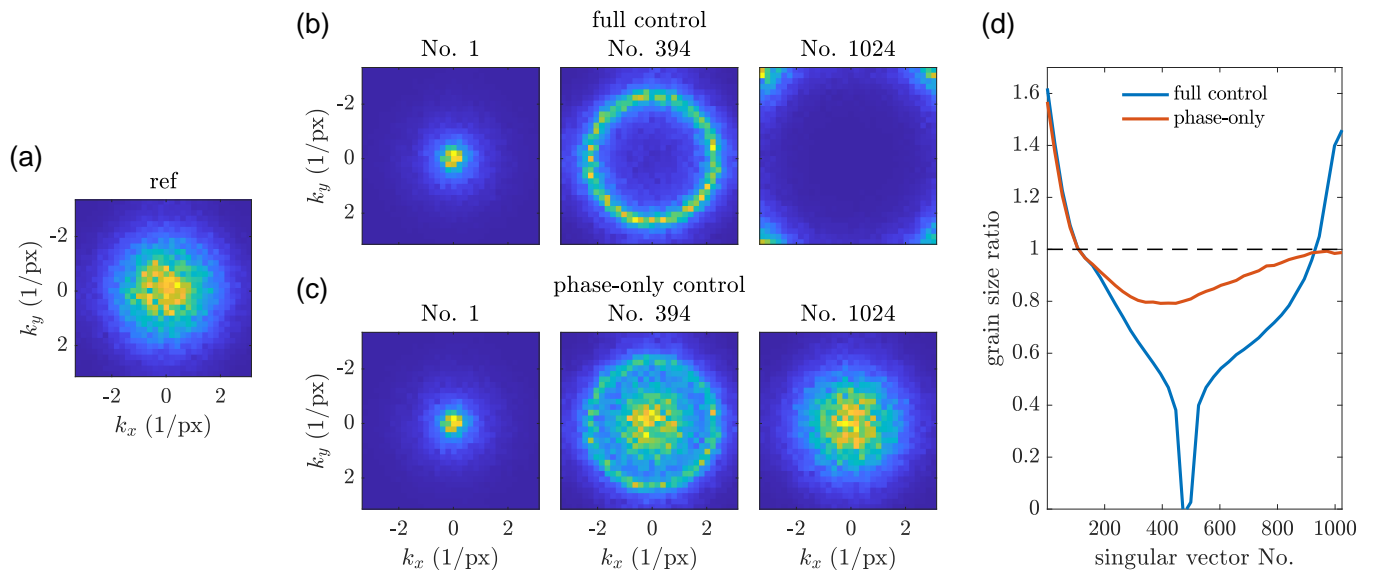


FIG. S2. Results from a minimal model of a random TM with local Gaussian correlations. A TM of size 1024×1024 was generated with a local correlation length of 2 pixels (FWHM) assuming a 32×32 output plane. (a) Shows the reference Fourier space distribution obtained for a random input pattern. (b) Shows the spatial frequency distribution of the output speckles when applying the first singular vector (left), an intermediate vector in the spectrum (middle) and the last vector (right). In (c) the same is shown assuming phase-only control at the input side. The speckle grain size enhancement ratio, extracted as in the experimental analysis, is presented in (d) for both the cases of full control (blue) and phase-only control (red). All results were averaged over 10 realizations of the TM.

the output speckle amplitudes obtained from the first singular vector, shown in Fig. 2(c). Here we perform a more thorough analysis of the phase distributions of the individual speckle realizations. Fig. S3 shows the individual output phase distributions of the first singular vector for a representative selection of realizations. For some realizations the speckles show a preferred phase, deviating from the statistics of a fully developed speckle. As discussed in the main text, we attribute this to the enhancement of the $|\vec{k}| = 0$ components of the field through the first singular vector. Note that even though the distribution can get peaked, it still spans the full phase range, generally regarded as a hallmark of fully developed speckles [1]. Also, since the phase peaks are randomly distributed, no preferred phase persists on average (see inset of Fig. 2(c)). Hence, on average also the first singular vector leads to Rayleigh distributed speckles with only small deviations of the amplitude distribution and the individual phase distributions, compatible with most applications requiring fully developed speckles.

Of the overall modes present in the medium we only control and measure a very limited fraction due to the small NA of the used objectives and the restriction to a single polarization state of the light. Therefore we are confident that the peaked phase distributions cannot stem from open channels or mesoscopic correlations [2].

IV. FILTERING TECHNIQUE

The filtering technique used is adapted from ref. [3] and is presented in Fig. S4. This filtering is solely numeric; no experimental changes need to be made to change from one filtering mask to another.

Note that, in contrast to [3], no decrease in efficiency is expected when filtering away more frequency components. In [3], after Fourier transforming the filtered k distribution back to real space, a single pixel was selected to focus on. However, after filtering, only a limited number of modes is available to interfere constructively at the focus site, reducing the efficiency compared to the unfiltered case. For the speckle engineering techniques presented here, on the other hand, the first singular vector concentrates the transmitted power in the targeted spatial modes without any further restrictions. When filtering more, the stronger reduction in the number of output modes only results in smaller transmission increase ratios for initial singular vectors.

To illustrate these points, we performed simulations and investigated the quality of the Bessel-like autocorrelation function for different widths w of the filtered ring (see Fig. S5). Here, no transformation back to real space after the Fourier filtering step was performed to demonstrate that in principle it is not necessary. Stronger filtering (small values of w) leads to more well-defined autocorrelation features without any apparent noise or background appearing

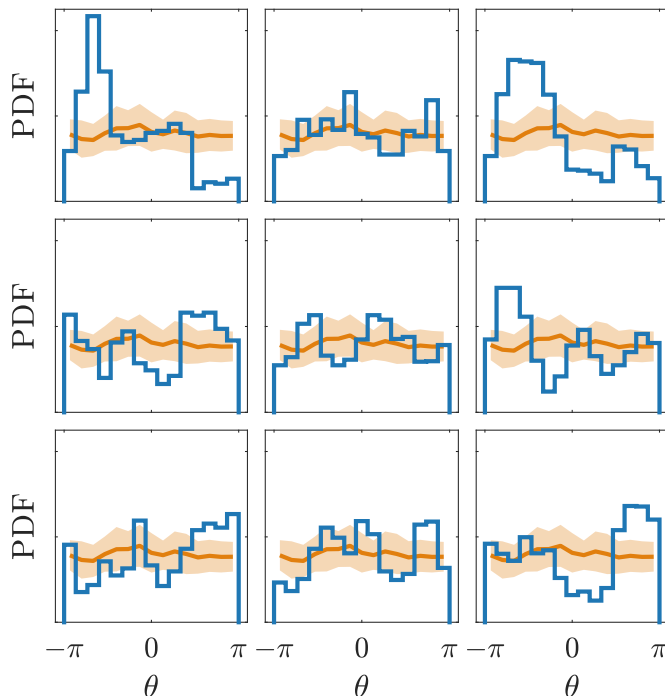


FIG. S3. Histogram showing the phase distributions for individual realizations of the output patterns obtained from displaying the first singular vectors. The data is the same as shown in Fig. 2, presenting 9 of the 36 realizations. The orange line gives the average distribution of the reference speckle with the shaded area marking one standard deviation.

as visible in Figs. S5(a,b): the speckle grains are visually narrower and the autocorrelation presents the characteristic enhance secondary maxima of a Bessel function. Also the fluctuations from realization to realization are not enhanced. However, as expected due to the reduction of the degrees of freedom in the output dimension of the filtered TM, the distribution of singular values changes and the overall transmission enhancement drops for more selective filtering masks (Fig. S5(c)).

V. ASYMMETRIC GRAINS THROUGH ONE-DIMENSIONAL SINGULAR VALUE DECOMPOSITION

In Fig. 3(b) of the main text we show how Fourier filtering can be used to create speckle patterns with asymmetric grains. Here we propose an alternative approach to realize such patterns which does not require any Fourier filtering. The idea is to apply the SVD only along one spatial dimension of the output region. In the TM, the columns associated to the individual pixels of the output region are not necessarily ordered. Exchanging two columns does not change the TM or the singular vector spectrum. The information which pixel is located next to which is contained only in the correlations between the TM elements. These correlations are also the source of the grain size dispersion observed in the output patterns of the singular vectors. Therefore, if we remove the correlations along one spatial dimension we can achieve the grain size enhancement along the remaining one only. To do so we divide the TM into sub-matrices which only encode the transmission for a single pixel row of the output field. Let us consider a TM of dimension $N_{\text{CCD}} \times N_{\text{SLM}}$, where N_{CCD} is the number of pixels in the output region-of-interest and N_{SLM} is the number of input modes controlled by the SLM. For simplicity we will assume a square region-of-interest such that the number of pixel rows at the output is $\sqrt{N_{\text{CCD}}}$. For each of these rows we obtain a sub-matrix of size $\sqrt{N_{\text{CCD}}} \times N_{\text{SLM}}$. The SVD is now performed separately on each of these sub-matrices, removing the correlations between the pixel rows from the process. Adding all resulting first singular vectors obtained from the individual decompositions constructs a mode that increases the grain size only along the spatial dimension associated to the output rows. The same procedure can of course be applied to the columns as well.

Fig. S6 shows the experimentally obtained speckles from the first singular vector of the regular SVD and the 1D SVD discussed above. In the case of the regular SVD the grains are enlarged in both x and y directions while for the one-dimensional SVD the elongation only happens in one direction leading to elongated speckle grains.

This technique gives good results and is easy to implement experimentally. The speckle elongation achieved is even

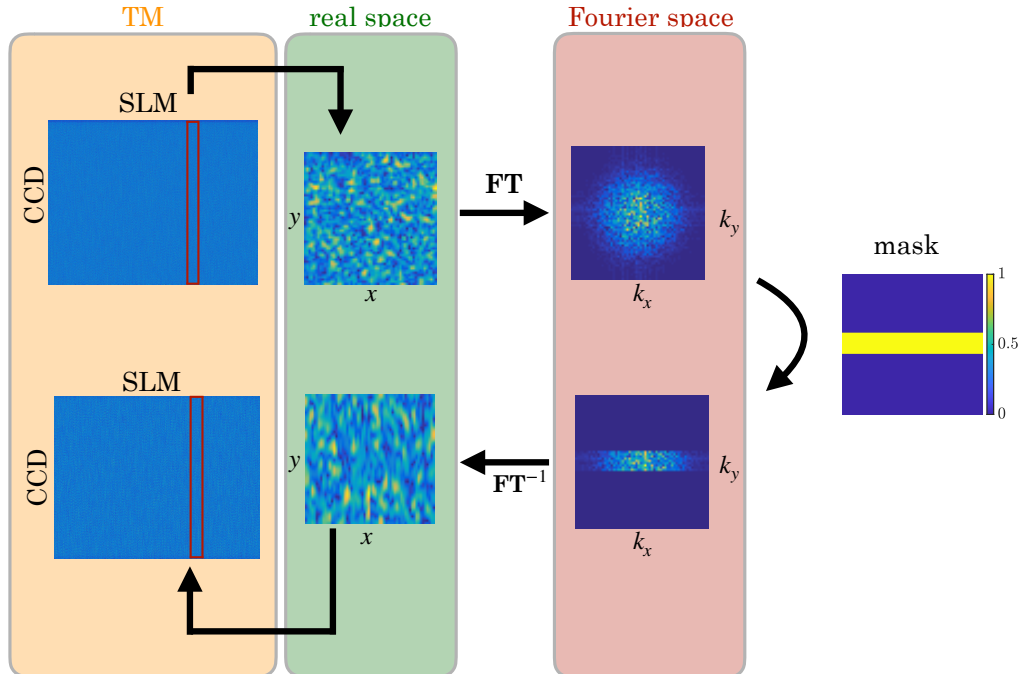


FIG. S4. Scheme of the TM filtering technique. For each input mode controlled at the SLM, the output field, represented by a column of the TM, is first reshaped in its original image configuration and then Fourier transformed (FT). After that, the Fourier representation is multiplied with a mask that selectively enhances or subdues certain k components (in the example shown the mask is binary). The modified field is transformed back to real space and reshaped into a column of the now filtered TM. The example TM shown here represents simulated data obtained from the model discussed above.

better than the one obtained by the filtering technique discussed in the main text. However, it allows only a specific deformation of the speckle grains while the filtering technique is much more versatile and intuitive.

VI. IMPACT OF THE DEGREE OF CONTROL

To complement the data shown in Fig. 2(b) of the main text we performed the same measurement for different amounts of control. As in Fig. 2, we image a plane at a distance ($z = 1$ mm) after the medium output surface. The number of modes controlled on the SLM is fixed to 1024 while a large region-of-interest is selected on the CCD camera. This region-of-interest is then successively subdivided into smaller ones of identical sizes to perform averaging. Measurements were taken with TMs of size 100×1024 , 225×1024 , 324×1024 and 900×1024 . Due to the subdivision of a fixed initial region-of-interest, the number of realizations averaged depends on the TM size (81, 36, 25 and 9 respectively), but is always realized over the same amount of speckle grains. The obtained results of the relative grain size evolution are presented in Fig. S7(a). The overall effect we observe is a smooth decrease from enhanced grain sizes for the initial singular vectors to smaller grains for intermediate vectors, followed by a return to the reference size. However, the amount of variation depends on the amount of control: the larger the ratio of controlled input modes to measured output modes the larger the variations achieved. In Fig. S7(b), plotting the relative grain size as a function of the field amplitude enhancement highlights an interesting point: the minimum grain size is obtained for $\eta_f = 1$. For lower enhancements $\eta_f < 1$ we observe a smooth evolution back to the reference grain size.

We observe that the exact shape of the relative grain size curves is dictated by the reference speckle k -space inhomogeneities. The common feature however is the smooth variation from enhancement to reduction, followed by a return to the reference size.

Note that we defined the grain size through the width of the autocorrelation of the amplitude speckle. This is done in order to be consistent with the experimental amplitude speckles displayed. However, defining the grain size through

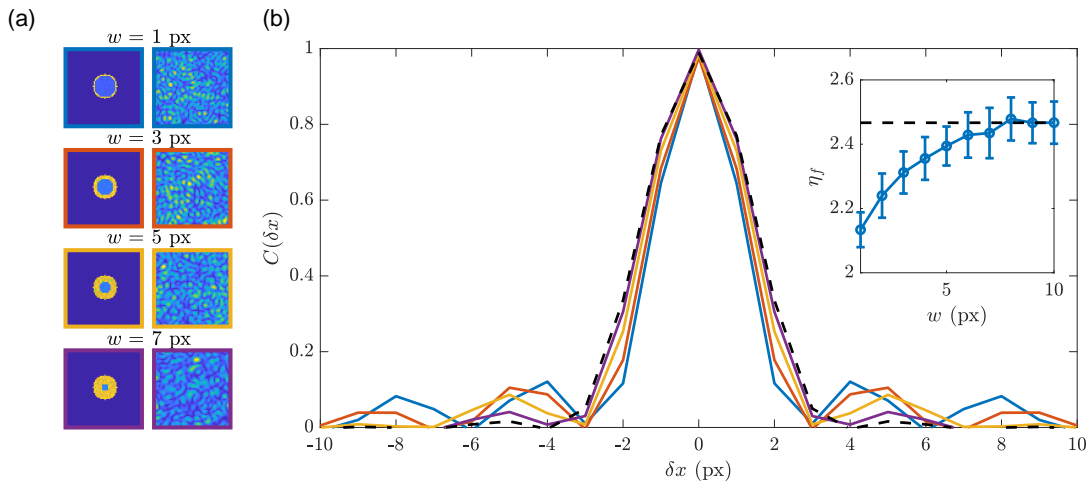


FIG. S5. Simulation of the filtering step impact on the noise. (a) Average Fourier transform of the fields behind the scattering medium (left) for different widths w of the filtering ring mask and examples of the associated speckles' field amplitudes (right). (b) Field autocorrelation (line colors correspond to the frame colors in (a)) and in inset the field enhancement of the first singular vector (No. 1) as a function of w for a complete set of masks. Error bars are given by the field enhancement standard deviation. The data are averaged over 50 realisations.

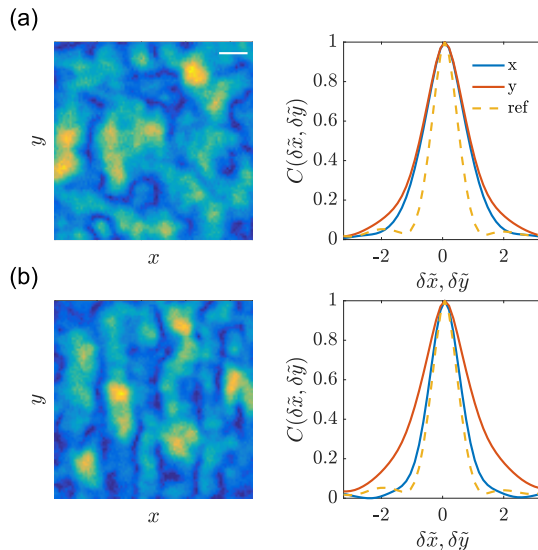


FIG. S6. Elongated speckles obtained from the one-dimensional SVD. Panel (a) shows the output for the first singular vector obtained from the regular SVD of the TM while (b) shows the output obtained from the 1D SVD. For both, an example of the output speckle amplitude (left, scale bars: $5 \mu\text{m}$) and the autocorrelation (right) are given. The autocorrelation is plotted along the x (blue) and y (red) directions and is compared to the reference speckle autocorrelation (orange dashed). The x -axes are rescaled by the FWHM of the reference speckle autocorrelation (see Fig. 3 caption). The autocorrelation curves are averaged over 9 realizations.

the intensity, the field amplitude or the field itself, gives the same relative grain sizes due to the normalization by the reference grain.

-
- [1] J. Goodman, *Speckle Phenomena in Optics: Theory and Applications* (Roberts & Company, 2007).
 [2] S. Rotter and S. Gigan, Light fields in complex media: Mesoscopic scattering meets wave control, *Reviews of Modern Physics* **89**, 015005 (2017).
 [3] A. Boniface, M. Mounaix, B. Blochet, R. Piestun, and S. Gigan, Transmission-matrix-based point-spread-function engineer-

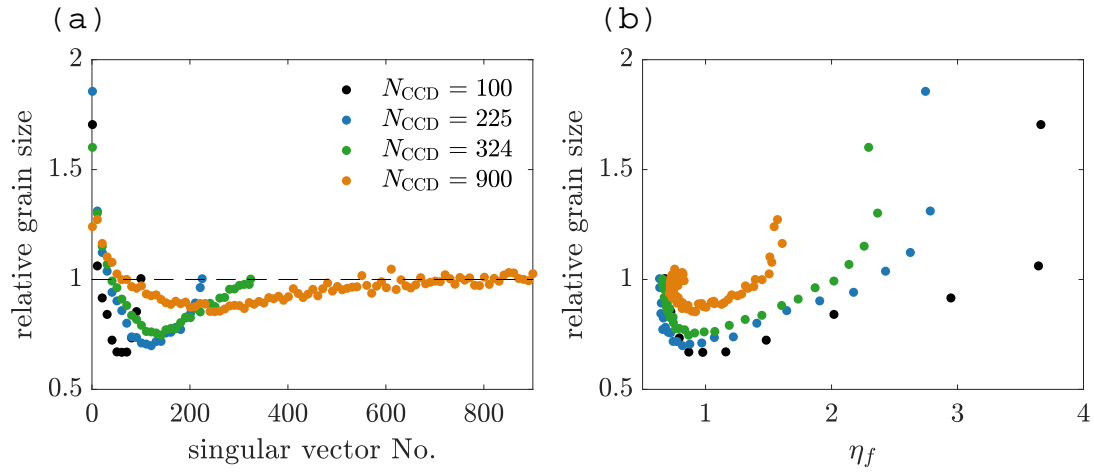


FIG. S7. Impact of the degree of control on the grain size control achieved with the SVD. (a) Relative grain size as a function of the singular vector number with the degree of control. The qualitative behavior remains the same while the amount of control scales range of the grain size variation. (b) Relative grain size as a function of the measured field enhancement η_f . Note that the minimum of the curve is always obtained for $\eta_f = 1$. All grain sizes values are averaged over the same number of grains, i.e. for the smaller region-of-interests more realizations are averaged.

ing through a complex medium, *Optica* **4**, 54 (2017).